Thorium(IV) and Uranium(IV) Ketimide Complexes Prepared by Nitrile Insertion into Actinide−Alkyl and −Aryl Bonds

Kimberly C. Jantunen, Carol J. Burns, Ingrid Castro-Rodriguez, Ryan E. Da Re,
Jeffery T. Golden, David E. Morris, Brian L. Scott, Felicia L. Taw, and
Jaqueline L. Kiplinger*

Chemistry Division, Los Alamos National Laboratory, Los Alamos, New Mexico 87545

Received December 17, 2003

Migratory insertion of benzonitrile into both An−C bonds of the bis(alkyl) and bis(aryl) complexes $(C_5Me_5)_2AnR_2$ yields the actinide ketimido complexes $(C_5Me_5)_2An[-N=C(Ph)(R)]_2$ (where An = Th, R = Ph, CH_2Ph, CH_3; An = U, R = CH_2Ph, CH_3) and provides a versatile method for the construction of electronically and sterically diverse ketimide ligands. The Th(IV) compounds represent the first examples of thorium ketimide complexes. The uranium complexes are surprisingly unreactive, and both the uranium and thorium bis(ketimido) complexes display unusual electronic structure properties. The combined chemical and physical properties of these complexes suggest a higher An−N bond order due to significant ligand-to-metal π-bonding in the actinide ketimido interactions and indicate that the f-electrons in mid-valent organouranium complexes might be far more involved in chemical bonding and reactivity than previously thought. We also report herein the structures of the known thorium and uranium complexes $(C_5Me_5)_2Th(CH_2Ph)_2$, $(C_5Me_5)_2ThMe_2$, $(C_5Me_5)_2U(CH_2Ph)_2$, and $(C_5Me_5)_2UMe_2$.

Introduction

The ketimide, or azavinylidene, functionality ($-N=CR_2$) has recently found increasing utility as an ancilliary ligand due to its steric and electronic flexibility (can serve as both a σ- and π-donor) and its ability to support a broad range of oxidation states for both d-block and f-block metals.[1−13] In fact, recent reports have shown that bulky ketimide ligands are instrumental for the preparation of novel diuranium inverted naphthalene and cyclooctatetraene sandwich complexes (**1**)[1] and organouranium complexes that exhibit oxidation state ambiguity (**2**).[2]

A variety of methods have proven useful in the synthesis of transition-metal and lanthanide ketimide complexes including, but not limited to, nucleophilic addition to coordinated nitrile ligands,[3] nitrile insertion into M−H, M−C, and M−Si bonds,[4] metathesis reactions between metal halides and alkali metal ketimide or 1-azallyl compounds,[1,5] addition of oximes and oxi-

* To whom correspondence should be addressed. Phone: 505-665-9553. Fax: 505-667-9905. E-mail: kiplinger@lanl.gov.

(1) Diaconescu, P. L.; Cummins, C. C. *J. Am. Chem. Soc.* **2002**, *124*, 7660−7661.

(2) Kiplinger, J. L.; Morris, D. E.; Scott, B. L.; Burns, C. J. *Organometallics* **2002**, *21*, 3073−3075.

(3) (a) Feng, S. G.; White, P. S.; Templeton, J. L. *J. Am. Chem. Soc.* **1994**, *116*, 8613−8620. (b) Kukushkin, V. Y.; Pombeiro, A. J. L. *Chem. Rev.* **2002**, *102*, 1771−1802, and references therein.

(4) (a) Evans, W. J.; Meadows, J. H.; Hunter, W. E.; Atwood, J. L. *J. Am. Chem. Soc.* **1984**, *106*, 1291−1300. (b) Erker, G.; Frömberg, W.; Atwood, J. L.; Hunter, W. E. *Angew. Chem., Int. Ed. Engl.* **1984**, *23*, 68−69. (c) Bercaw, J. E.; Davies, D. L.; Wolczanski, P. T. *Organometallics* **1986**, *5*, 443−450. (d) Jordan, R. F.; Bajgur, C. S.; Dasher, W. E.; Rheingold, A. L. *Organometallics* **1987**, *6*, 1041−1051. (e) Bochmann, M.; Wilson, L. M.; Hursthouse, M. B.; Motevalli, M. *Organometallics* **1988**, *7*, 1148−1154. (f) Woo, W. G.; Tilley, T. D. *J. Organomet. Chem.* **1990**, *393*, C6−C9. (g) Debad, J. D.; Legzdins, P.; Lumb, S. A.; Batchelor, R. J.; Einstein, F. W. B. *Organometallics* **1992**, *11*, 6−8. (h) Erker, G.; Pfaff, R.; Kowalski, D.; Würthwein, E. U.; Krüger, C.; Goddard, R. *J. Org. Chem.* **1993**, *58*, 6771−6778. (i) Temme, B.; Erker, G.; Frölich, R.; Grehl, M. *J. Chem. Soc., Chem. Commun.* **1994**, 1713−1714. (j) Debad, J. D.; Legzdins, P.; Lumb, S. A.; Batchelor, R. J.; Einstein, F. W. B. *Organometallics* **1995**, *14*, 2543−2555. (k) Erker, G.; Ahlers, W.; Fröhlich, R. *J. Am. Chem. Soc.* **1995**, *117*, 5853−5854. (l) Armstrong, D. R.; Henderson, K. W.; Little, I.; Jenny, C.; Kennedy, A. R.; McKeown, A. E.; Mulvey, R. E. *Organometallics* **2000**, *19*, 4369−4375. (m) For a photochemically induced nitrile insertion into a Ta−CH_3 bond, see: Boring, E.; Sabat, M.; Finn, M. G.; Grimes, R. *Organometallics* **1997**, *16*, 3993−4000.

(5) (a) Collier, M. R.; Lappert, M. F.; McMeeking, J. *Inorg. Nucl. Chem. Lett.* **1971**, *7*, 689−694. (b) Erker, G.; Frömberg, W.; Krüger, C.; Raabe, E. *J. Am. Chem. Soc.* **1988**, *110*, 2400−2405. (c) Zhang; S.; Piers, W. E. *Organometallics* **2001**, *20*, 2088−2092.

(6) (a) Werner, H.; Knaup, W.; Dziallas, M. *Angew. Chem., Int. Ed. Engl.* **1987**, *26*, 248−250. (b) Werner, H.; Daniel, T.; Müller, M.; Mahr, M. *J. Organomet. Chem.* **1996**, *512*, 197−205. (c) Ferreira, C. M. P.; Guedes da Silva, M. F.; Kukushkin, V. Y.; Fraústo da Silva, J. J. R.; Pombeiro, A. J. L. *J. Chem. Soc., Dalton Trans.* **1998**, 325−326.

(7) (a) Zippel, T.; Arndt, P.; Ohff, A.; Spannenberg, A.; Kempe, R.; Rosenthal, U. *Organometallics* **1998**, *17*, 4429−4437.

(8) (a) Lefeber, C.; Arndt, P.; Tillack, A.; Baumann, W.; Kempe, R.; Burlakov, V. V.; Rosenthal, U. *Organometallics* **1995**, *14*, 3090−3093. (b) Hou, Z.; Yoda, C.; Koizumi, T.; Nishiura, M.; Wakatsuki, Y.; Fukuzawa, S.; Takats, J. *Organometallics* **2003**, *22*, 3586−3592, and references therein.
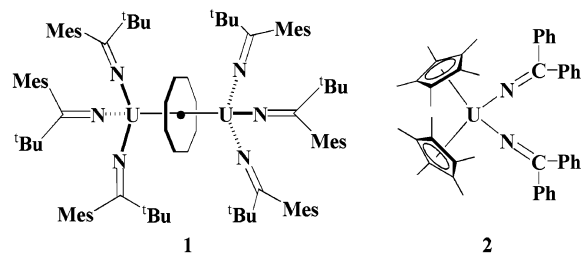
(9) Tsai, Y. C.; Stevens, F. H.; Meyer, K.; Mendiratta, A.; Gheorghiu, M. D.; Cummins, C. C. *Organometallics* **2003**, *22*, 2902−2913.

(10) (a) Colquhoun, H. M.; Crease, A. E.; Taylor, S. A.; Williams, D. J. *J. Chem. Soc., Dalton Trans.* **1988**, 2781−2786. (b) Merzweiler, K.; Fenske, D.; Hartmann, E.; Dehnicke, K. *Z. Naturforsch.* **1989**, *44b*, 1003−1006. (c) Redshaw, C.; Wilkinson, G.; Hussain-Bates, B.; Hursthouse, M. B. *J. Chem. Soc., Dalton Trans.* **1992**, 555−562. (d) Mommertz, A.; Leo, R.; Massa, W.; Dehnicke, K. *Z. Naturforsch.* **1998**, *53b*, 887−892. (e) Tanabe, Y.; Seino, H.; Ishii, Y.; Hidai, M. *J. Am. Chem. Soc.* **2000**, *122*, 1690−1699.
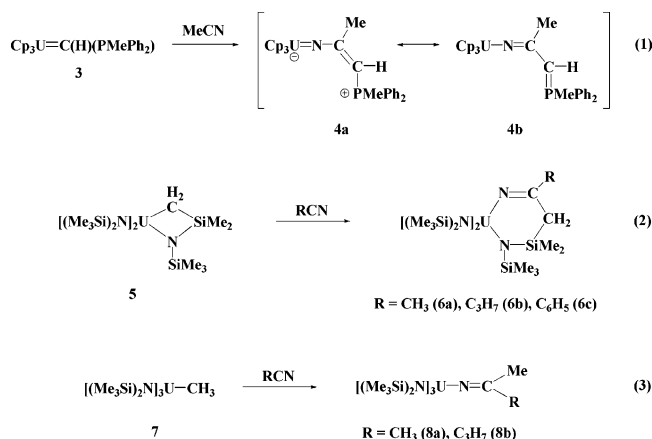
(11) Cramer, R. E.; Panchanatheswaran, K.; Gilje, J. W. *J. Am Chem. Soc.* **1984**, *106*, 1853−1854.

(12) Dormond, A.; Aaliti, A.; Elbouadili, A.; Moise, C. *J. Organomet. Chem.* **1987**, *329*, 187−199.

(13) Dormond, A.; Aaliti, A.; El Bouadili, A.; Moise, C. *Inorg. Chim. Acta* **1987**, *139*, 171−176.
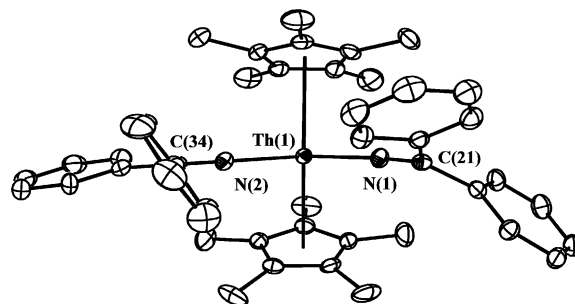
Figure 1. Molecular structure of **10a** with thermal ellipsoids at the 25% probability level. Selected bond distances (Å) and angles (deg): Th(1)−N(1) 2.259(4), Th(1)−N(2) 2.265(5), N(1)−C(21) 1.259(7), N(2)−C(34) 1.272(7), C(21)−N(1)−Th(1) 174.0(4), C(34)−N(2)−Th(1) 179.4(5), N(1)−Th(1)−N(2) 108.95(17).

mate salts to electron-rich metal centers,[6] reductive cleavage of azines,[2,7] and reductive coupling of both Schiff bases[8] and nitriles.[9,10] Compared to the transition-metal ketimides, actinide ketimide complexes are rare; only a handful of examples possessing a uranium metal center have been reported. The ketimide ligands in complex **1** were introduced using metathesis chemistry and in complex **2** by the reductive cleavage of benzophenone azine. The remaining examples consist of the uranium mono(ketimide) complexes **4**,[11] **6**,[12] and **8**[12,13] prepared by nitrile insertion into U=C, U−CH$_2$, and U−CH$_3$ bonds, respectively.

$$Cp_3U=C(H)(PMePh_2) \xrightarrow{MeCN} \left[\begin{array}{c} Cp_3U=N-C \\ 4a \end{array} \leftrightarrow \begin{array}{c} Cp_3U-N=C \\ 4b \end{array} \right] \quad (1)$$

3

$$[(Me_3Si)_2N]_2U \xrightarrow{RCN} [(Me_3Si)_2N]_2U \quad (2)$$

5

R = CH$_3$ (**6a**), C$_3$H$_7$ (**6b**), C$_6$H$_5$ (**6c**)

$$[(Me_3Si)_2N]_3U-CH_3 \xrightarrow{RCN} [(Me_3Si)_2N]_3U-N=C \quad (3)$$

7

R = CH$_3$ (**8a**), C$_3$H$_7$ (**8b**)

The above examples represent the body of work currently known for ketimide chemistry of the actinide metals. To the best of our knowledge, there are no previous reports of thorium ketimide complexes.

In our effort to explore valence ambiguity in organometallic actinide chemistry[2] and develop synthetic entries into actinide complexes containing multiply bonded functional groups,[14] we devised a general high-yield method for preparation of actinide bis(ketimide) compounds. We now report that benzonitrile inserts into thorium−alkyl and −aryl bonds in complexes of the type (C$_5$Me$_5$)$_2$ThR$_2$ to afford the first examples of thorium ketimido complexes (C$_5$Me$_5$)$_2$Th[−N=C(Ph)(R)]$_2$ (where R = Ph, CH$_2$Ph, CH$_3$). This chemistry can be readily extended to the preparation of uranium bis(ketimide) complexes, (C$_5$Me$_5$)$_2$U[−N=C(Ph)(R)]$_2$ (where R = CH$_2$Ph, CH$_3$), and constitutes a generalized method for the construction of electronically and sterically diverse ketimide ligands. Herein, we describe the syntheses, structures, and properties of these thorium(IV) and uranium(IV) bis(ketimido) complexes. In addition, we also present the structures for the known thorium and uranium complexes, (C$_5$Me$_5$)$_2$Th(CH$_2$Ph)$_2$, (C$_5$Me$_5$)$_2$-

(14) (a) Arney, D. S. J.; Burns, C. J. *J. Am. Chem. Soc.* **1995**, *117*, 9448−9460, and references therein. (b) Warner, B. P.; Scott, B. L.; Burns, C. J. *Angew. Chem., Int. Ed.* **1998**, *37*, 959−960.

ThMe$_2$, (C$_5$Me$_5$)$_2$U(CH$_2$Ph)$_2$, and (C$_5$Me$_5$)$_2$UMe$_2$, as these complexes are useful starting materials for the preparation of many organometallic actinide complexes, yet their molecular structures have not been reported.

Results and Discussion

Synthesis and Structural Characterization of Thorium and Uranium Ketimide Complexes. As depicted in eq 4, treatment of a colorless toluene solution of (C$_5$Me$_5$)$_2$ThPh$_2$ (**9a**) with excess benzonitrile instantly generates the highly iridescent orange-colored thorium(IV) bis(ketimido) complex **10a**, which was isolated as an orange crystalline solid in 82% yield.

$$\quad (4)$$

R = Ph, **9a**, **10a**; CH$_2$Ph, **9b**, **10b**; CH$_3$, **9c**, **10c**.
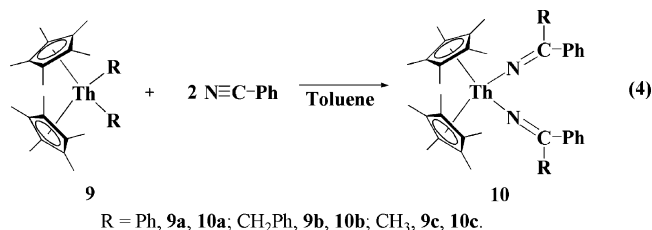
Reaction of **9b** and **9c** with benzonitrile similarly affords the bright yellow colored thorium(IV) bis(ketimido) complexes **10b** (72% isolated yield) and **10c** (75% isolated yield), respectively. It is important to note that reaction of **9a** with acetonitrile (N≡C−CH$_3$) also gives the bis(ketimido) complex **10c**, further illustrating the generality of this synthetic method for the construction of ketimide ligands. The modest isolated yields reflect the high solubility of the ketimide complexes rather than the formation of any byproducts. When the reactions are monitored by ^{1}H NMR spectroscopy, compounds **10a**−**c** are the only observable thorium-containing products and are formed in yields greater than 95%. All compounds display sharp NMR resonances consistent with a diamagnetic 6d^{0}5f^0 Th(IV) metal center being present.

A single-crystal X-ray diffraction study of complex **10a** (Figure 1) revealed that benzonitrile inserted into both Th−C bonds of (C$_5$Me$_5$)$_2$ThPh$_2$ (**9a**) in a 1,2-fashion to form two new nitrogen bonds to the thorium metal center. The Th−N−C angles are nearly linear (174.0(4)°, 179.4(5)°) and the Th−N distances (2.259(4) Å, 2.265(5) Å) are shorter on average by ca. 0.1 Å than those observed for other thorium amide complexes (e.g., (η^3-
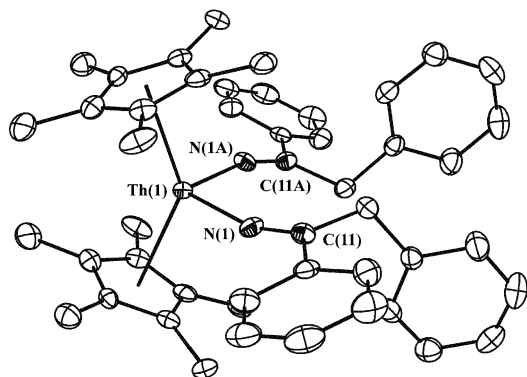
Figure 2. Molecular structure of **10b** with thermal ellipsoids at the 25% probability level. Selected bond distances (Å) and angles (deg): Th(1)−N(1) 2.256(8), N(1)−C(11) 1.264(13), C(11)−N(1)−Th(1) 161.2(8), N(1)−Th(1)−N(1A) 102.9(4).

$BH_4)Th[N(SiMe_3)_2]_3$, Th−N_{av} = 2.32(2) Å;[15a] $(C_5Me_5)_2$-Th(Cl)$(C_6H_8N_3)$, Th−N_{av} = 2.46(1) Å;[15b] $(\eta^8$-$C_8H_8)$Th-$[N(SiMe_3)_2]_2$, Th−N_{av} = 2.34(1) Å;[15c] Th$[N(SiMe_3)_2]_2$-$(NMePh)_2$, Th−N_{av} = 2.308(7) Å[15d]. An interesting comparison is provided by the structurally related Th(IV) imido complex $(C_5Me_5)_2$Th(=N-2,6-$Me_2C_6H_3$)-(THF), which possesses a Th=N bond distance of 2.045(8) Å and a Th−N−C bond angle of 171.5(7)°.[16] In complex **10a**, the planes defined by N(1)=C(21)$(C_{ipso})_2$ and N(2)=C(34)$(C_{ipso})_2$ are nearly orthogonal (110.6° and 84.9°, respectively) to the $Cp_{(centroid)}$−Th−$Cp_{(centroid)}$ (Cp = C_5Me_5) plane. The N=C bond lengths (1.259(7) Å; 1.272(7) Å) are consistent with sp²-hybridization[17] and compare well with those found in other structurally characterized ketimido complexes.[1−10] In total, all of the structural features suggest that there is ligand-to-metal π-bonding in both thorium ketimido interactions.

The molecular structure of complex **10b** (Figure 2) is nearly identical to that for **10a** except that it displays a bent geometry at the ketimide nitrogens (Th−N−C 161.2(8)°). This bending may simply be a manifestation of unfavorable steric interactions. Similar to **10a**, the Th−N distances (2.256(8) Å) in complex **10b** are significantly shorter compared to other structurally characterized thorium amide complexes.[15] As such, shortening of the Th−N bond distances due to sp-hybridization cannot be ruled out.

The nitrile insertion chemistry was successfully applied to the synthesis of uranium bis(ketimide) complexes. Reaction of the bis(alkyl) uranium complexes **11b** and **11c** with excess benzonitrile affords the dark red uranium(IV) bis(ketimido) complexes **12b** (88% isolated yield) and **12c** (71% isolated yield), respectively (eq 5).

As with the thorium systems, the modest isolated yields observed for the uranium compounds reflect the high solubility of the ketimide complexes rather than the formation of any byproducts. When the reactions

R = Ph, **11a**; CH_2Ph, **11b**, **12b**; CH_3, **11c**, **12c**.
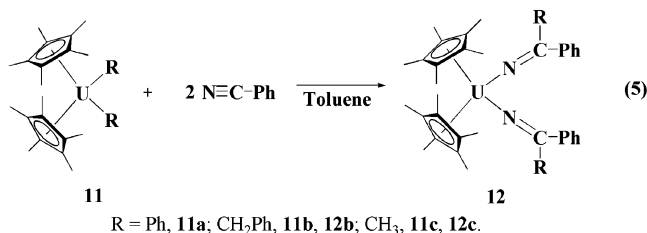
are monitored by ¹H NMR spectroscopy, compounds **12b,c** are the only observable uranium-containing products and are formed in yields greater than 95%. Furthermore, the NMR spectra for **12b,c** are sharp and paramagnetically shifted, suggesting that the complexes retain the U(IV) oxidation state.[18]

In contrast to the thorium chemistry, the reaction between $(C_5Me_5)_2UPh_2$ (**11a**) and benzonitrile does not give the bis(ketimide) complex $(C_5Me_5)_2U(−N=CPh_2)_2$ (**2**), and instead leads to an intractable mixture of products. This marked difference in reactivity may be explained by analogy to previous observations that solutions of the uranium diphenyl derivative **11a** eliminate benzene at room temperature.[19] The formation of benzyne intermediates in this system has been postulated in the preparation of a uranindene complex (**14**), prepared from the insertion of diphenylacetylene into one of the two U−C bonds of the transient $(C_5Me_5)_2U$-(benzyne) (**13**) species (eq 6).
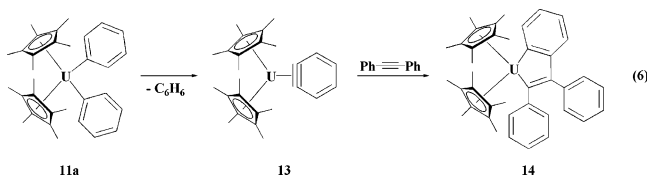
The thorium analogue **9a** undergoes the same transformation as in eq 6; however, temperatures of 100 °C are required to achieve rates comparable to the uranium system at room temperature.[19]

As mentioned above, earlier reports demonstrated that under the appropriate conditions, organonitriles insert into uranium−carbon bonds to give uranium ketimide functional groups (eqs 1−3).[11−13] In all three examples, only a single uranium−carbon bond was elaborated to give a ketimide functional group. For complex **5**, ring strain is clearly a factor in promoting the nitrile insertion chemistry to give the six-membered metallacycles **6a−c**.[12] Whereas nitrile insertion into the U−CH_3 bond in **7** could be achieved under mild conditions,[13] insertion of acetonitrile into the U=C bond of **3** required elevated temperatures to give the unusual uranium ketimide complex **4**.[11] Thus, the chemistry in this report is distinctive in that it demonstrates that nitrile insertion chemistry (1) is not limited to uranium alkyl complexes and (2) can take place at more than one uranium−carbon or thorium−carbon bond using readily accessible actinide alkyl derivatives to furnish a broad range of actinide bis(ketimide) complexes.

The X-ray structure of the uranium bis(ketimide) complex **2** was previously reported.[2] This complex was

(15) Turner, H. W.; Andersen, R. A.; Zalkin, A.; Templeton, D. H. *Inorg. Chem.* **1979**, *18*, 1221−1224. (b) Sternal, R. S.; Sabat, M.; Marks, T. J. *J. Am. Chem. Soc.* **1987**, *109*, 7920−7921. (c) Gilbert, T. M.; Ryan, R. R.; Sattelberger, A. P. *Organometallics* **1988**, *7*, 2514−2518. (d) Barnhart, D. M.; Clark, D. L.; Grumbine, S. K.; Watkin, J. G. *Inorg. Chem.* **1995**, *34*, 1695−1699.
(16) Haskel, A.; Straub, T.; Eisen, M. *Organometallics* **1996**, *15*, 3773−3775.
(17) Allen, F. H.; Kennard, O.; Watson, D. G.; Brammer, L.; Orpen, A. G.; Taylor, R. *J. Chem. Soc., Perkin Trans. 2* **1987**, S1−S19.

(18) (a) Marks, T. J.; Kolb, J. R. *J. Am. Chem. Soc.* **1975**, *97*, 27−33. (b) Marks, T. J. *Prog. Inorg. Chem.* **1979**, *25*, 223−333.
(19) Fagan, P. J.; Manriquez, J. M.; Maatta, E. A.; Seyam, A. M.; Marks, T. J. *J. Am. Chem. Soc.* **1981**, *103*, 6650−6667.
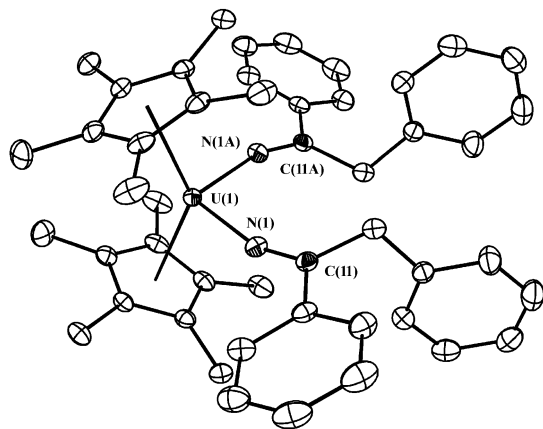
Figure 3. Molecular structure of **12b** with thermal ellipsoids at the 25% probability level. Selected bond distances (Å) and angles (deg): U(1)−N(1) 2.184(3), N(1)−C(11) 1.274(4), C(11)−N(1)−U(1) 162.4(3), N(1)−U(1)−N(1A) 102.40(15).

prepared by the reaction of $(C_5Me_5)_2UCl_2$ with two reducing equivalents (provided by KC_8), followed by addition of 1 equiv of benzophenone azine, $Ph_2C=N−N=CPh_2$. Complex **2** is isostructural to the thorium derivative **10a**; any significant deviation in the M−N bond distances between the two complexes is readily attributable to the smaller ionic radius of U(IV) versus Th(IV).[20] Important structural parameters are the U−N distances of 2.179(6) and 2.185(5) Å, the N=C distances of 1.293(8) and 1.281(8) Å, and the U−N−C bond angles of 173.4(6)° and 176.5(5)°. These are consistent with the formulation of the ligands as ketimide groups with the uranium metal center accepting density from the nitrogen 2p lone-pairs.

As noted for the thorium bis(ketimide) derivatives, the molecular structure of complex **12b** (Figure 3) is nearly identical to that of **2** except that it displays a significantly more bent geometry at the ketimide nitrogens (U−N−C 162.4(3)°). Similar to **2**, the U−N distances (2.184(3) Å) in complex **12b** are significantly shorter compared to other structurally characterized uranium(IV) amide complexes (e.g., $Cp_3U[N(C_6H_5)_2]$, U−N = 2.29(1) Å;[21a] $(C_5Me_5)_2U[NH(2,6-Me_2C_6H_3)]_2$, U−N = 2.267(6) Å;[21b] $(C_5Me_5)(\eta^5-C_5Me_4CH_2NAd)U[NH-(Ad)]$, U−N = 2.231(6), 2.155(7) Å;[21c] $(C_5Me_5)_2U\{\eta^3-(N,N',N')-[N(H)(2,4-^tBu_2C_6H_2-6-CH_2−N−N=CPh_2)]\}$, U−N = 2.315(9), 2.228(10) Å;[14c] $[Me_2Si(\eta^5-C_5Me_4)(^tBuN)]U(NMe_2)_2$, U−N = 2.278(4), 2.207(4), 2.212(4) Å[21d]). The short U−N bond distances and nearly linear U−N−C bond angles in complexes **2** and **12b** are consistent with significant uranium−nitrogen multiple-bond character and compare favorably with other uranium(IV) ketimide (e.g., $(DME)(I)U[−N=C(^tBu)(2,4,6-Me_3C_6H_2)]_3$,[1] U−N = 2.176(12), 2.196(12), 2.196(13) Å, U−N−C = 171.4(17)°, 160.4(13)°, 172.8(14)°, and $Cp_3U−N=C(Me)CH-(PMePh_2)$,[11] U−N = 2.06(1) Å, U−N−C = 163(1)°) and uranium(IV) sulfilimine (e.g., $(C_5Me_5)_2U(−N−SPh_2)_2$,[22] U−N = 2.143(3) Å, U−N−S = 152.2(2)°) complexes

which have been described as containing significant π-bonding between the uranium and nitrogen. For comparison purposes, it is useful to note that complexes **2** and **12b** are reminiscent of high-valent uranium(VI) bis(imido) complexes, which have significant uranium-imido multiple-bond character as illustrated by the complex $(C_5Me_5)_2U(=N−Ph)_2$, which exhibits a U−N−C bond angle of 177.8(6)° and U−N = 1.952(7) Å.[23] However, the metal center in complexes **2** and **12b** is not U(VI), but is clearly U(IV) on the basis of comparison of the U−N bond distances in the two systems as well as the NMR and UV−visible−near-IR spectra (vide infra).

Further evidence for a higher U−N bond order in the U(IV) ketimido interactions is provided by their chemistry, which is distinct from known U(IV) amide complexes. For example, we previously noted that complex **2** displays no reaction chemistry with substrates such as benzophenone, phenylacetylene, diphenylacetylene, carbon monoxide, pyridine *N*-oxide, or dihydrogen.[2] This lack of reactivity is in marked contrast to observations by Marks and Eisen, who have shown that uranium(IV) amide complexes of the type $(C_5Me_5)_2U(NR'R)_2$ readily insert carbon monoxide to form bis(carbamoyl) complexes $(C_5Me_5)_2U(\eta^2-CONR'R)_2$,[24] as well as undergo amine elimination upon reaction with phenylacetylene to generate the bis(acetylide) complex $(C_5Me_5)_2U(−C\equiv C−Ph)_2$.[21b]

The thorium and uranium ketimide complexes possess markedly different chemical properties. A survey of the reactivity of **10a** indicates that the Th−N linkage is reactive toward Ph−C≡C−H and pyridine-*N*-oxide as evidenced by the formation of benzophenone imine. This is clearly distinct from the analogous uranium ketimido system (**2**), which displays no reaction chemistry toward identical substrates as noted above. Furthermore, the mass spectrometry for the uranium and thorium ketimide systems may provide some insight into the nature of the bonding in the U−N and Th−N linkages. Whereas the thorium ketimide complexes are unstable and do not produce a discernible mass spectrum, the uranium ketimide mass spectrometry fragmentation pattern reveals loss of C_5Me_5 rather than loss of $N=CPh_2$, providing further evidence for the robust character of the $U(−N=CPh_2)_2$ core. These observations suggest that there are important differences in the ketimido ligand N(2p) lone-pair π-bonding interactions with U(IV) versus Th(IV), and therefore in the degree of multiple bonding between the ketimide ligand and U(IV) and Th(IV) metal centers.[25]

Electronic Structural Characterization of the Thorium and Uranium Ketimide Complexes. The structural data described above demonstrate that the interaction between the tetravalent actinide metals and the ketimide ligands involves some degree of π-bonding to account for the relative shortening of the metal−

(20) Shannon, R. D. *Acta Crystallogr., Sect. A* **1976**, *A32*, 751−767.
(21) (a) Cramer, R. E.; Engelhardt, U.; Higa, K. T.; Gilje, J. W. *Organometallics* **1987**, *6*, 41−45. (b) Straub, T.; Frank, W.; Reiss, G. J.; Eisen, M. S. *J. Chem. Soc., Dalton Trans.* **1996**, 2541−2546. (c) Peters, R. G.; Warner, B. P.; Scott, B. L.; Burns, C. J. *Organometallics* **1999**, *18*, 2587−2589. (d) Stubbert, B. D.; Stern, C. L.; Marks, T. J. *Organometallics* **2003**, *22*, 4836−4838.

(22) Ariyaratne, K. A. N. S.; Cramer, R. E.; Gilje, J. W. *Organometallics* **2002**, *21*, 5799−5802.
(23) Arney, D. S. J.; Burns, C. J.; Smith, D. C. *J. Am. Chem. Soc.* **1992**, *114*, 10068−10069.
(24) Fagan, P. J.; Manriquez, J. M.; Vollmer, S. H.; Day, C. S.; Day, V. W.; Marks, T. J. *J. Am. Chem. Soc.* **1981**, *103*, 2206−2220.
(25) Further studies employing techniques such as PES will be of interest for probing the degree of multiple bonding between the ketimide ligand and U(IV)/Th(IV). For example, see: Brennan, J. G.; Green. J. C.; Redfern, C. M. *Inorg. Chim. Acta* **1987**, *139*, 331−333.
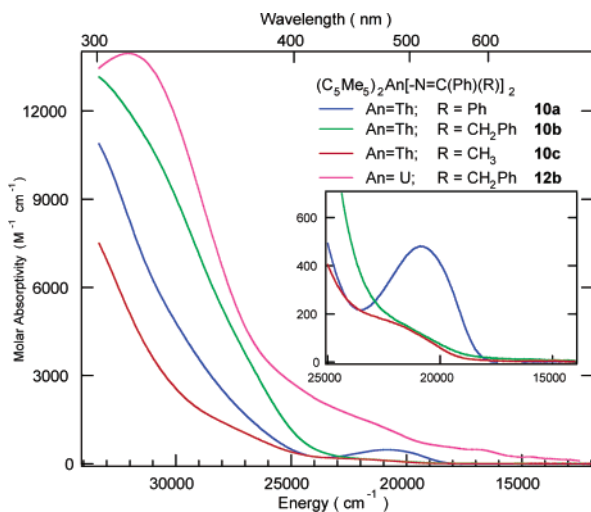
Figure 4. Electronic absorption spectra of $\sim 1 \times 10^{-4}$ M toluene solutions of $(C_5Me_5)_2Th[-N=C(Ph)(R)]_2$ (**10a**, R = Ph, blue; **10b**, R = CH_2Ph, green; **10c**, R = CH_3, red) and $(C_5Me_5)_2U[-N=C(Ph)(CH_2Ph)]_2$ (**12b**, pink).

nitrogen bonds. The resulting enhanced electronic interaction between the metal and ligands should also be reflected in probes of electronic structure, namely, electronic absorption spectroscopy and cyclic voltammetry. The vivid colors exhibited by the Th(IV) ketimido complexes (**10a**−**c**) are clearly reflected in the UV−visible electronic absorption spectra (Figure 4). These complexes all possess broad, intense electronic absorption bands that extend from the UV into the visible wavelength range, with an additional weak feature between 450 and 500 nm (Figure 4). The spectrum of $(C_5Me_5)_2U[-N=C(Ph)(CH_2Ph)]_2$ (**12b**) is included in Figure 4 for comparison. This complex has similarly intense, broad absorption bands throughout the UV−visible region, but in addition possesses weaker and somewhat more structured broad bands that tail to lower energy. These additional lower-energy transitions render the U(IV) complex a dark red color. (This complex also has numerous f−f bands in the near-infrared (not shown in Figure 4) derived from the $5f^2$ electronic configuration.)[26]

Most Th(IV) complexes are colorless, reflecting the absence of valence electrons on the metal center ($6d^05f^0$ electronic configuration). There have been a few reports of colored Th(IV) organometallic species, and the color in these complexes has been attributed to visible ligand-to-metal charge-transfer (LMCT) transitions.[27] Thorium(III) complexes, while relatively rare, are intensely colored because the $6d^15f^0$ or $6d^05f^1$ electronic configurations engender ligand field (d−d or f−f) or electric dipole-allowed metal-localized (f−d) transitions.[28] Interestingly, the structurally related d^0 early transition metal ketimido complexes $(C_5H_5)_2M(-N=CPh_2)_2$ (M = Ti, Zr) are also highly colored (red in both cases); however, no electronic spectral data have been
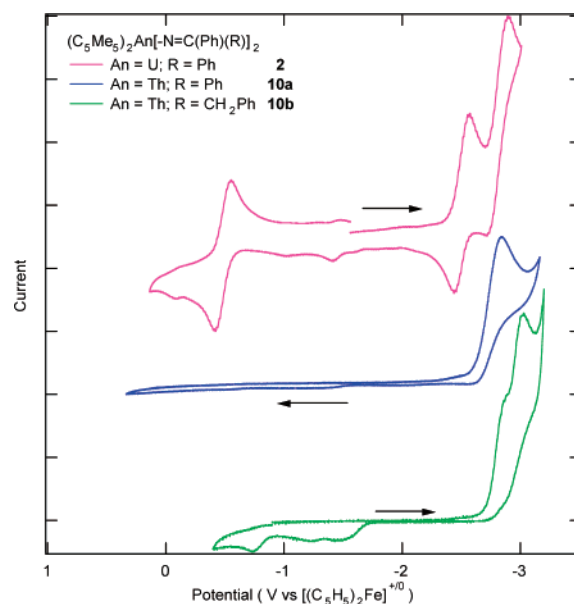

Figure 5. Cyclic voltammograms of $\sim 5 \times 10^{-3}$ M solutions of $(C_5Me_5)_2Th[-N=C(Ph)(R)]_2$ (**10a**, R = Ph, blue; **10b**, R = CH_2Ph, green) and $(C_5Me5)_2U(-N=CPh_2)_2$ (**2**, pink) in 0.1 M $[(n-Bu_4N][B(C_6F_5)_4]$/THF at a Pt electrode. Scan rate is 200 mV/s.

reported for these and the origin of the color has not been ascribed to any specific electronic transition.[4b,7] The high molar absorptivity values found for these Th(IV) and U(IV) ketimido complexes in the UV−visible region are consistent with ligand-localized $\pi-\pi^*$ and/or charge-transfer transitions. In fact, the molar absorptivity in this spectral region for other $(C_5Me_5)_2An$-(R)(R′) complexes where R, R′ = alkyl or aryl seldom exceeds about 5000 M^{-1} cm^{-1} at the short wavelength limit of the solvent.[26] Thus, the more intense bands seen for the ketimido complexes must be attributable to new electronic states derived from transitions into or out of high-lying ligand-based orbitals. We have also observed visible luminescence from these Th(IV) ketimido complexes and resonance-enhanced Raman vibrational spectra from both the Th(IV) and U(IV) ketimido systems. The existence of these more molecular-type spectral properties is quite unusual, even for the early actinide metals and their complexes other than the actinyl (AnO_2^{n+}) species that possess metal−oxygen multiple bonds. However, such properties are consistent with enhanced electronic interactions between the actinide and the ketimido ligands. Complete details of this novel molecular-spectroscopic behavior will be provided in a forthcoming paper.[29]

The cyclic voltammetric data for the ketimido complexes (Figure 5) reflect the novel electronic structure in two important ways. First, although the Th(IV) complexes do not possess voltammetric waves attributable to metal-based redox processes, they do possess ketimido ligand-based reduction waves. This demonstrates the existence of empty low-lying ligand-based acceptor orbitals that are available to participate as the terminal orbitals in an optical excitation process as seen in the absorption spectral data. Second, the U(IV) ketimido complexes (such as **2** shown in Figure 5)

(26) Morris, D. E.; Da Re, R. E.; Jantunen, K. C.; Castro-Rodriguez, I.; Kiplinger, J. L. *Organometallics*, in press.

(27) Cloke, F. G. N.; Hitchcock, P. B. *J. Am. Chem. Soc.* **1997**, *119*, 7899−7900.

(28) (a) Kaltsoyannis, N.; Bursten, B. E. *J. Organomet. Chem.* **1997**, *528*, 19−33. (b) Parry, J. S.; Cloke, F. G. N.; Coles, S. J.; Hursthouse, M. B. *J. Am. Chem. Soc.* **1999**, *121*, 6867−6871. (c) Blake, P. C.; Edelstein, N. M.; Hitchcock, P. B.; Kot, W. K.; Lappert, M. F.; Shalimoff, G. V.; Tian, S. *J. Organomet. Chem.* **2001**, *636*, 124−129.

(29) Da Re, R. E.; Jantunen, K. C.; Golden, J. T.; Kiplinger, J. L.; Morris, D. E., manuscript in preparation.
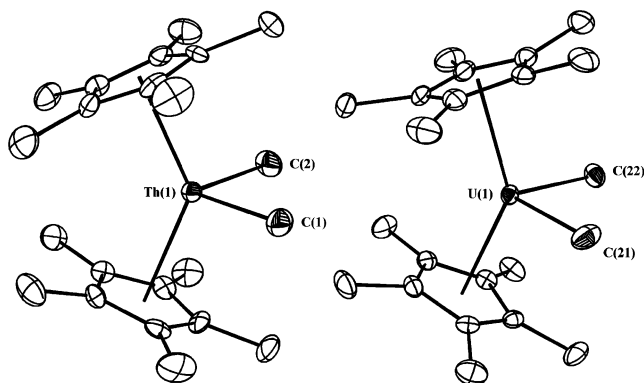
Figure 6. Molecular structures of complexes **9c** (left) and **11c** (right) with thermal ellipsoids at the 25% probability level. Selected bond distances (Å) and angles (deg) for **9c**: Th(1)−C(1) 2.471(8); Th(1)−C(2) 2.478(9); C(1)−Th(1)−C(2) 98.6(4); Th−C$_{cent}$ 2.518; Th−C$_{ring(av)}$ 2.792(6); C$_5$Me$_{5(cent)}$−Th−C$_5$Me$_{5(cent)}$ 133.9. Selected bond distances (Å) and angles (deg) for **11c**: U(1)−C(21) 2.424(7); U(1)−C(22) 2.414(7); C(21)−U(1)−C(22) 94.5(3); U−C$_{cent}$ 2.456, 2.461; U−C$_{ring(av)}$ 2.732(7), 2.739(6); C$_5$Me$_{5(cent)}$−U−C$_5$Me$_{5(cent)}$ 140.5.

exhibit reversible redox waves associated with metal-based reduction [U(IV)/U(III)] and oxidation [U(V)/U(IV)]. While the reduction process is quite common for U(IV) organometallic complexes, the presence of an electrochemically reversible oxidation wave to generate a U(V) species is rare.[30] The stabilization of the U(V) oxidation state appears to be a direct consequence of the additional π-bonding interaction between the actinide metal and the ketimido ligands.[26]

Structural Characterization of the Thorium and Uranium Complexes (C$_5$Me$_5$)$_2$ThMe$_2$ (9c), (C$_5$Me$_5$)$_2$UMe$_2$ (11c), (C$_5$Me$_5$)$_2$Th(CH$_2$Ph)$_2$ (9b), and (C$_5$Me$_5$)$_2$U(CH$_2$Ph)$_2$ (11b). In the course of our studies on thorium(IV) and uranium(IV) bis(ketimide) complexes, we obtained single crystals of the known complexes **9b,c** and **11b,c** suitable for X-ray diffraction.[31] The molecular structures of these widely used actinide starting materials have not been reported. As illustrated in Figure 6, the molecular structures of **9c** and **11c** reveal a typical bent metallocene framework with a pseudotetrahedral coordination environment about the thorium and uranium atoms, respectively. The complexes are isostructural; any significant deviation between the M−C bond distances exhibited by the two complexes is readily attributable to the smaller ionic radius of U(IV) versus Th(IV).[20] Within the metallocene wedge lie the two methyl ligands (Th(1)−C(1) 2.471(8) Å, Th(1)−C(2) 2.478(9) Å, C(1)−Th(1)−C(2) 98.6(4)° for **9c** and U(1)−C(21) 2.424(7) Å, U(1)−C(22) 2.414(7) Å, C(21)−U(1)−C(22) 94.5(3)° for **11c**). The metrical parameters in these

complexes are as expected; the Th−CH$_3$ and U−CH$_3$ bond distances compare favorably with those found in other structurally characterized thorium(IV) and uranium(IV) methyl complexes (e.g., Cp$_2$Th(dmpe)(CH$_3$)$_2$, Th−C = 2.583(7), 2.562(8) Å;[32a] (C$_5$Me$_5$)$_2$Th[P(SiMe$_3$)$_2$]-(CH$_3$), Th−C = 2.510(13) Å;[32b] (C$_{11}$H$_{11}$)$_3$Th(CH$_3$), Th−C = 2.48(3), 2.50(3) Å;[32c] (C$_9$Me$_7$)$_2$Th(CH$_3$)$_2$, Th−C = 2.48(2), 2.47(2) Å;[32d] (dmpe)U(CH$_2$Ph)$_3$(CH$_3$), U−C = 2.41(1) Å;[33a] [PhC(NSiMe$_3$)$_2$]$_3$U(CH$_3$), U−C = 2.498(5) Å;[33b] [1,3-(Me$_3$Si)$_2$C$_5$H$_3$]$_2$U(CH$_3$)$_2$, U−C = 2.42(2) Å;[33c] [(3,5-Me$_2$C$_6$H$_3$)(^{t}Bu)N]$_3$U(CH$_3$), U−C = 2.446(7) Å;[33d] [(C$_5$Me$_5$)$_2$U(OSO$_2$CF$_3$)(CH$_3$)]$_2$, U−C$_{av}$ = 2.416(7) Å[33e]).

Figure 7 illustrates the molecular structures of complexes **9b** and **11b**. As with the methyl derivatives, these complexes are isostructural; any significant deviation between the M−C bond distances exhibited by the two complexes is readily attributable to the smaller ionic radius of U(IV) versus Th(IV).[20] If one ignores the short U(1)−C(22) and Th(1)−C(22) contacts, the geometry of the complexes is pseudotetrahedral about the actinide metal centers. In both **9b** and **11b**, the actinide(IV) metal center is bound to the pentamethylcyclopentadienyl ligands in an η^5-manner and the two benzyl ligands are positioned in the equatorial girdle of the (C$_5$Me$_5$)$_2$-An (An = Th, U) bent metallocene framework. One of the benzyl ligands is bound to the metal center in an η^1-fashion (complex **11b**, benzyl ligand #1: U(1)−C(28) = 2.467(5) Å, U(1)−C(29) = 3.656(5) Å, U(1)−C(28)−C(29) = 134.2(4)°; complex **9b**, benzyl ligand #1: Th(1)−C(28) = 2.551(7) Å, Th(1)−C(29) = 3.709(6) Å, Th(1)−C(28)−C(29) = 133.0(6)°) and displays no secondary interactions between the arene ring and the actinide metal center. The second benzyl ligand is bound to the actinide metal center in a multihapto fashion as clearly demonstrated by the metrical parameters associated with the uranium- and thorium-benzyl linkages (complex **11b**, benzyl ligand #2: U(1)−C(21) = 2.489(5) Å, U(1)−C(22) = 2.970(5) Å, U(1)−C(21)−C(22) = 93.6(3)°, U(1)−C(23) = 3.605(6) Å, U(1)−C(27) = 3.581(6) Å; complex **9b**, benzyl ligand #2: Th(1)−C(21) = 2.552(7) Å, Th(1)−C(22) = 2.979(6) Å, Th(1)−C(21)−C(22) = 91.7(4)°, Th(1)−C(23) = 3.622(7) Å, Th(1)−C(27) = 3.556(6) Å). These benzyl groups are best described as η^4 with the strongest secondary interaction occurring between the actinide metal center and the ipso carbon of the coordinated benzyl ligand, in addition to weaker unsymmetrical secondary interactions taking place between the actinide metal and the ortho carbons of the benzyl ligand.

(30) (a) Clappe, C.; Leveugle, D.; Hauchard, D.; Durand, G. *J. Electroanal. Chem.* **1998**, *448*, 95−103. (b) Hauchard, D.; Cassir, M.; Chivot, J.; Ephritikhine, M. *J. Electroanal. Chem.* **1991**, *313*, 227−241. (c) Hauchard, D.; Cassir, M.; Chivot, J.; Baudry, D.; Ephritikhine, M. *J. Electroanal. Chem.* **1993**, *347*, 399−407. (d) Schnabel, R.; Scott, B.; Smith, W.; Burns, C. *J. Organomet. Chem.* **1999**, *591*, 14−23. (e) Sonnenberger, D. C.; Gaudiello, J. G. *Inorg. Chem.* **1988**, *27*, 2747−2748. (f) Ossola, F.; Zanella, P.; Ugo, P.; Seeber, R. *Inorg. Chim. Acta* **1988**, *147*, 123−126. (g) Finke, R. G.; Gaughan, G.; Voegeli, R. *J. Organomet. Chem.* **1982**, *229*, 179−184.
(31) Fagan, P. J.; Manriquez, J. M.; Maatta, E. A.; Seyam, A. M.; Marks, T. J. *J. Am. Chem. Soc.* **1981**, *103*, 6650−6667.

(32) (a) Zalkin, A.; Brennan, J. G.; Andersen, R. A. *Acta Crystallogr.* **1987**, *C43*, 418−420. (b) Hall, S. W.; Huffman, J. C.; Miller, M. M.; Avens, L. R.; Burns, C. J.; Arney, D. S. J.; England, A. F.; Sattelberger, A. P. *Organometallics* **1993**, *12*, 752−758. (c) Spirlet, M. R.; Rebizant, J.; Bettonville, S.; Goffart, J. *Acta Crystallogr.* **1993**, *C49*, 1138−1140. (d) Trnka, T. M.; Bonanno, J. B.; Bridgewater, B. M.; Parkin, G. *Organometallics* **2001**, *20*, 3255−3264.
(33) (a) Edwards, P. G.; Andersen, R. A.; Zalkin, A. *Organometallics* **1984**, *3*, 293−298. (b) Wedler, M.; Knösel, F.; Edelmann, F. T.; Behrens, U. *Chem. Ber.* **1992**, *125*, 1313−1318. (c) Lukens, W. W., Jr.; Beshouri, S. M.; Blosch, L. L.; Stuart, A. L.; Andersen, R. A. *Organometallics* **1999**, *18*, 1235−1246. (d) Diaconescu, P. L.; Odom, A. L.; Agapie, T.; Cummins, C. C. *Organometallics* **2001**, *20*, 4993−4995. (e) Kiplinger, J. L.; John, K. D.; Morris, D. E.; Scott, B. L.; Burns, C. J. *Organometallics* **2002**, *21*, 4306−4308.
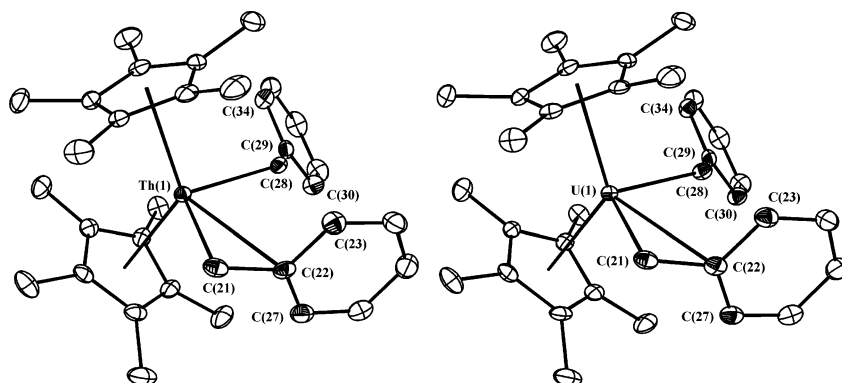
Figure 7. Molecular structures of complexes **9b** (left) and **11b** (right) with thermal ellipsoids at the 25% probability level. Selected bond distances (Å) and angles (deg) for complex **9b**: Th(1)−C(21) 2.552(7); Th(1)−C(28) 2.551(7); Th(1)−C(22) 2.979(6); Th(1)−C(29) 3.709(6); Th(1)−C(23) 3.622(7); Th(1)−C(27) 3.556(6); Th(1)−C(30) 4.700(6); Th(1)−C(34) 4.341(6); Th−C_{cent} 2.564, 2.577; Th−C_{ring} 2.836(8), 2.843(8); Th(1)−C(21)−C(22) 91.7(4); Th(1)−C(28)−C(29) 133.0(6); C(21)−Th(1)−C(28) 108.4(3); $C_5Me_{5(cent)}$−Th−$C_5Me_{5(cent)}$ 131.4. Selected bond distances (Å) and angles (deg) for complex **11b**: U(1)−C(21) 2.489(5); U(1)−C(28) 2.467(5); U(1)−C(22) 2.970(5); U(1)−C(29) 3.656(5); U(1)−C(23) 3.605(6); U(1)−C(27) 3.581(6); U(1)−C(30) 4.675(5); U(1)−C(34) 4.292(5); U−C_{cent} 2.492, 2.514; U−C_{ring} 2.768(5), 2.787(6); U(1)−C(21)−C(22) 93.6(3); U(1)−C(28)−C(29) 134.2(4); C(21)−U(1)−C(28) 107.55(18); $C_5Me_{5(cent)}$−U−$C_5Me_{5(cent)}$ 131.5.

Table 1. Bond Lengths (Å) in Actinide Benzyl Complexes

compound	MC_{ipso}−MCH_2[a]	MC_o−MCH_2[b]	$MC_{o'}$−MCH_2[c]	Δ[d]	Δ'[e]	ref
(dmpe)U(CH$_2$Ph)$_3$(Me)[f] (shortest contacts)	0.22	0.55	0.91	0.33	0.69	33a
(dmpe)Th(CH$_2$Ph)$_4$[f] (shortest contacts)	0.35	0.78	0.39	0.43	0.58	33a
(C$_5$Me$_5$)U(CH$_2$Ph)$_3$ (shortest contacts)	0.34	0.89	0.94	0.56	0.61	34b
(C$_5$Me$_5$)Th(CH$_2$Ph)$_3$ (shortest contacts)	0.29	0.77	1.00	0.48	0.71	34a
(C$_5$Me$_5$)$_2$Th(CH$_2$Ph)$_2$ (**9b**) (benzyl ligand #1, Th−CH$_2$ = Th(1)−C(28))	1.16	1.79	2.15	0.63	0.99	this work
(C$_5$Me$_5$)$_2$Th(CH$_2$Ph)$_2$ (**9b**) (benzyl ligand #2, Th−CH$_2$ = Th(1)−C(21))	0.43	1.00	1.11	0.58	0.68	this work
(C$_5$Me$_5$)$_2$U(CH$_2$Ph)$_2$ (**11b**) (benzyl ligand #1, U−CH$_2$ = U(1)−C(28))	1.19	1.83	2.21	0.64	1.02	this work
(C$_5$Me$_5$)$_2$U(CH$_2$Ph)$_2$ (**11b**) (benzyl ligand #2, U−CH$_2$ = U(1)−C(21))	0.48	1.09	1.12	0.61	0.64	this work

[a] Metal-to-ipso carbon bond length minus metal-to-methylene carbon bond length. [b] Metal-to-shorter ortho carbon bond length minus metal-to-methylene carbon bond length. [c] Metal-to-longer ortho carbon bond length minus metal-to-methylene carbon bond length. [d] [MC_o − MCH_2] − [MC_{ipso} − MCH_2]. [e] [$MC_{o'}$ − MCH_2]. [f] dmpe = 1,2-bis(dimethyldiphosphino)ethane.

The propensity for benzyl ligands to bond in an η^4-mode with actinide metals has been previously noted.[33a,34] These interactions are relatively weak and are a manifestation of the requirement of large electropositive actinide metals to maximize their coordination numbers and to minimize the intramolecular ligand−ligand repulsions; the resulting molecular structure is a compromise between these two conflicting tendencies. Two parameters have been defined by Marks[33a] and Andersen[34a] to quantify the benzyl ligand-to-metal interaction, Δ and Δ', where Δ = [MC_o − MCH_2] − [MC_{ipso} − MCH_2] and Δ' = [$MC_{o'}$ − MCH_2] − [MC_{ipso} − MCH_2] and where MC_o is the shorter metal-to-ortho carbon contact, $MC_{o'}$ is the longer metal-to-ortho contact, MCH_2 is the metal-to-methylene carbon bond length, and MC_{ipso} is the metal-to-ipso carbon bond length. For the f-block metals, Δ and Δ' have been shown to have comparable values, as would be expected for an η^4-benzyl-to-metal bonding interaction. Table 1 compares and contrasts the Δ and Δ' values determined for complexes **9b** and **11b** with the other structurally characterized actinide benzyl complexes that exhibit η^4-benzyl-to-metal bonding interactions. The metrical parameters exhibited by complexes **9b** and **11b** support the assignment of η^1 and η^4 hapticity for the benzyl ligands in these complexes.

Concluding Remarks

In conclusion, we have reported a convenient method for the construction of electronically and sterically diverse ketimide ligands and demonstrated its efficacy through the preparation of a variety of novel thorium(IV) and uranium(IV) bis(ketimido) complexes. The thorium compounds represent the first examples of thorium ketimide complexes. The uranium complexes are surprisingly unreactive, and both the uranium and thorium bis(ketimido) complexes display unusual electronic structure properties. The combined chemical and physical properties of these complexes suggest an An−N bond order greater than 1 due to significant ligand-to-metal π-bonding in the actinide ketimido interactions. For the uranium complexes, these data are suggestive of electronic delocalization throughout the N−U−N core in the uranium(IV) bis(ketimide) systems and indicate that the f-electrons in mid-valent organouranium com-

(34) (a) Mintz, E. A.; Moloy, K. G.; Marks, T. J.; Day, V. W. *J. Am. Chem. Soc.* **1982**, *104*, 4692−4695. (b) Kiplinger, J. L.; Morris, D. E.; Scott, B. L.; Burns, C. J. *Organometallics* **2002**, *21*, 5978−5982.

plexes might be far more involved in chemical bonding and reactivity than previously thought.

Experimental Section

General Procedures. Unless otherwise noted, reactions and manipulations were performed at 20 °C in a recirculating Vacuum Atmospheres Model HE-553-2 inert atmosphere (N_2 or He) drybox with a MO-40-2 Dri-Train, or using standard Schlenk and high vacuum line techniques. Glassware was dried overnight at 150 °C before use. All NMR spectra were obtained using a Bruker Avance 300 MHz spectrometer. Except when noted, NMR spectra were acquired at room temperature (25 °C). Benzene-d_6 and toluene-d_8 were obtained from Cambridge Isotope Laboratories (CIL). Chemical shifts were referenced to protio solvent impurities (δ 7.14 for benzene-d_6 and δ 2.05 for toluene-d_8), which are referenced to internal $Si(CH_3)_4$ at δ 0.00 ppm.

Melting points were determined with a Mel-Temp capillary melting point apparatus equipped with a Fluke 51 II K/J thermocouple using capillary tubes flame-sealed under nitrogen; values are uncorrected. Mass spectrometric (MS) analyses were obtained at the University of California, Berkeley Mass Spectrometry Facility, using either VG ProSpec (EI) or VG70-SE (FAB) mass spectrometers. Elemental analyses were performed at the University of California, Berkeley Microanalytical Facility, on a Perkin-Elmer Series II 2400 CHNS analyzer.

Electronic absorption spectral data were obtained for toluene solutions of all complexes over the wavelength range from 300 to 1600 nm on a Perkin-Elmer Model Lambda 19 UV−visible−near-infrared spectrophotometer. All data were collected in 1 cm path length cuvettes loaded in an inert atmosphere glovebox and run versus a toluene reference. Strong absorption bands from overtone vibrations of the toluene solvent precluded the collection of data at wavelengths longer than 1600 nm, but samples were run separately versus air references to ensure that the observed absorption bands were attributable to the complexes and not the solvent. Samples were run at two dilutions, 0.1 and 0.5 mM, to optimize absorbance in the UV−visible and near-infrared, respectively. Spectral resolution was typically 2 nm in the visible region and 4−6 nm in the near-infrared.

Cyclic voltammetric data were obtained in the Vacuum Atmospheres drybox system described above. All data were collected using a Perkin-Elmer Princeton Applied Research Corporation (PARC) Model 263 potentiostat under computer control with PARC Model 270 software. All sample solutions were ~5 mM in complex with 0.1 M $[(n\text{-}C_4H_9)_4N][B(C_6F_5)_4]$ supporting electrolyte in THF solvent. This electrolyte has been shown previously to greatly diminish the solution resistance in low-dielectric solvents such as THF. All data were collected with the positive-feedback IR compensation feature of the software/potentiostat activated to ensure minimal contribution to the voltammetric waves from uncompensated solution resistance (typically ~1 kΩ under the conditions employed). Solutions were contained in PARC Model K0264 microcells consisting of an ~3 mm diameter Pt disk working electrode, a Pt wire counter electrode, and a silver wire quasi-reference electrode. Scan rates from 20 to 5000 mV/s were employed to assess the chemical and electrochemical reversibility of the observed redox transformations. Potential calibrations were performed at the end of each data collection cycle using the ferrocenium/ferrocene couple as an internal standard.

Both electronic absorption data and cyclic voltammetric data were analyzed using Wavemetrics IGOR Pro (Version 4.0) software on a Macintosh platform.

Materials. Unless otherwise noted, reagents were purchased from commercial suppliers and used without further purification. Celite (Aldrich) and alumina (Brockman I, Ald-

rich) were dried in vacuo at 250 °C for 48 h prior to use. Anhydrous toluene (Aldrich), hexanes (Aldrich), diethyl ether (Aldrich), and tetrahydrofuran (Aldrich) were passed through a column of activated alumina (A2, 12 × 32, Purifry) under nitrogen and stored over activated 4 Å molecular sieves prior to use.

Benzonitrile (Aldrich) and acetonitrile (Aldrich) were distilled from CaH_2 and stored over activated 4 Å molecular sieves under N_2 prior to use. $(C_5Me_5)_2Th(Ph)_2$ (**9a**),[35] $(C_5Me_5)_2Th(CH_2\text{-}Ph)_2$ (**9b**),[31] $(C_5Me_5)_2Th(CH_3)_2$ (**9c**),[31] $(C_5Me_5)_2U(CH_2Ph)_2$ (**11b**),[31] and $(C_5Me_5)_2U(CH_3)_2$ (**11c**)[31] were prepared according to literature procedures. Deuterated solvents were purified by storage over activated 4 Å molecular sieves or sodium metal prior to use.

Synthesis of $(C_5Me_5)_2Th(-N=CPh_2)_2$ (10a). A 125 mL Erlenmeyer flask equipped with a stir bar was charged with $(C_5Me_5)_2Th(C_6H_5)_2$ (0.38 g, 0.57 mmol) and toluene (50 mL). To the resulting colorless solution was added 0.13 mL of benzonitrile (0.131 g, 1.26 mmol) with stirring. The reaction mixture changed color to a bright orange solution and was stirred at room temperature for 15 h. The resultant mixture was filtered through a Celite-padded coarse frit. The filtrate was collected, and the volatiles were removed under reduced pressure to give an orange crystalline solid. The solid was collected by filtration, washed with hexanes (2 × 10 mL), and dried in vacuo to afford crude **10a** as an orange crystalline solid. Analytically pure samples of **10a** were obtained by recrystallization from hot hexanes (0.453 g, 0.419 mmol, 82%). ^{1}H NMR (C_6D_6, 298 K): δ 7.64 (dd, 8H, meta H), 7.17 (d, $J = 2.2$ Hz, 8H, ortho H), 1.96 (s, 30H, $C_5(CH_3)_5$). The para proton on the phenyl ring is unobserved in the ^{1}H NMR (this was also evident in a {C, H} 2D-COSY experiment). ^{13}C{^{1}H} NMR (C_6D_6, 298 K): δ 173.72 (s, ($-N=CPh_2)_2$), 144.21 (s, quat aryl C), 129.21, 129.10, 128.44 (aryl Cs), 123.73 (s, $C_5(CH_3)_5$), 11.67 (s, $C_5(CH_3)_5$). UV−vis/NIR (ϵ, M^{-1} cm^{-1}, toluene): 300 (10 900), 333 (4800), 480 (480). Mp = 187−189 °C. Anal. Calcd for $C_{46}H_{50}N_2Th$ (862.96 g/mol): C, 64.02; H, 5.84; N, 3.25. Found: C, 63.91; H, 5.88; N, 3.31.

Synthesis of $(C_5Me_5)_2Th[-N=C(Ph)(CH_2Ph)]_2$ (10b). A 125 mL Erlenmeyer flask equipped with a stir bar was charged with $(C_5Me_5)_2Th(CH_2Ph)_2$ (0.50 g, 0.73 mmol) and toluene (50 mL). To the resulting pale yellow solution was added 0.149 mL of benzonitrile (0.150 g, 1.46 mmol) with stirring. The resultant reaction mixture changed color to a bright yellow and was stirred at room temperature for 12 h. The resultant mixture was filtered through a Celite-padded coarse frit. The filtrate was collected, and the volatiles were removed under reduced pressure to give a yellow solid. The solid was collected by filtration, washed with hexanes (3 × 10 mL), and dried in vacuo to afford crude **10b** as a yellow solid. Analytically pure samples of **10b** were obtained by recrystallization from a concentrated hexanes solution at −30 °C (0.468 g, 0.525 mmol, 72%). ^{1}H NMR (C_6D_6, 298 K): δ 7.79 (d, 4H, ortho H (phenyl), 7.31 (d, 4H, ortho H (benzyl)), 7.02 (m, 12 H, meta/para H), 4.14 (br s, 4H, CH_2Ph), 2.03 (s, 30H, $C_5(CH_3)_5$). UV−vis/NIR (ϵ, M^{-1} cm^{-1}, toluene): 300 (13,150), 463 (155). Mp = 178−182 °C. Anal. Calcd for $C_{55}H_{59}N_3Th$ (994.13 g/mol): C, 66.45; H, 5.98; N, 4.23. Found: C, 66.10; H, 6.09; N, 4.18.

Synthesis of $(C_5Me_5)_2Th[-N=C(Ph)(CH_3)]_2$ (10c). Method A. A 125 mL Erlenmeyer flask equipped with a stir bar was charged with $(C_5Me_5)_2Th(CH_3)_2$ (1.42 g, 2.66 mmol) and toluene (50 mL). To the resulting colorless solution was added 0.656 mL of benzonitrile (0.663 g, 6.43 mmol) with stirring. The resultant reaction mixture changed color to bright yellow and was stirred at room temperature for 48 h. The resultant mixture was filtered through a Celite-padded coarse frit. The filtrate was collected, and the volatiles were removed under reduced pressure to give a yellow oil. The oil was

(35) England, A. F.; Burns, C. J.; Buchwald, S. L. *Organometallics* **1994**, *13*, 3491−3495.

triturated sequentially with pentanes (3 × 10 mL) and hexanes (3 × 10 mL) to give a bright yellow powder, which was dried in vacuo to afford analytically pure **10c** as a yellow solid (1.46 g, 1.99 mmol, 75%). ^{1}H NMR (C_6D_6, 298 K): δ 7.85 (m, 4H, ortho H), 7.24 (m, 6H, meta/para H), 2.41 (s, 6H, CH_3), 1.99 (s, 30H, C_5(CH_3)$_5$). UV−vis/NIR (ϵ, M^{-1} cm^{-1}, toluene): 300 (7,500), 345 (1,770), 452 (165). Mp = 178−182 °C. Anal. Calcd for $C_{36}H_{46}N_2$Th·1/2C_6H_{14} (781.89 g/mol): C, 59.91; H, 6.83; N, 3.58. Found: C, 60.01; H, 6.69; N, 3.27.

Synthesis of (C₅Me₅)₂Th[−N=C(Ph)(CH₃)]₂ (10c). Method B. A 5 mm Teflon NMR tube insert seated inside a 5 mm glass NMR tube was charged with (C₅Me₅)₂Th(C₆H₅)₂ (0.024 g, 3.65 × 10^{-5} mol) and 0.5 mL of C_6D_6. A syringe was used to introduce 4 μL of acetonitrile. Immediately upon addition of the acetonitrile, the solution surface region was noted to turn bright yellow. The Teflon NMR liner was sealed with a Teflon plug and the glass NMR tube capped with a plastic cap. The resulting apparatus was shaken vigorously to ensure thorough mixing of the solution. Over a period of 5 min the solution slowly changed color from nearly colorless to a bright yellow clear solution. ^{1}H NMR experiments show the product is identical to **10c** (apparent quant. yield). ^{1}H NMR (C_6D_6, 298 K): δ 7.85 (m, 4H, ortho H), 7.24 (m, 6H, meta/para H), 2.41 (s, 6H, CH_3), 1.99 (s, 30H, C_5(CH_3)$_5$).

Synthesis of (C₅Me₅)₂U[−N=C(Ph)(CH₂Ph)]₂ (12b). A 125 mL Erlenmeyer flask equipped with a stir bar was charged with (C₅Me₅)₂U(CH₂Ph)₂ (0.50 g, 0.73 mmol) and toluene (50 mL). To the resulting green-black solution was added 0.195 mL of benzonitrile (0.197 g, 1.91 mmol) with stirring. The resultant mixture changed color to a red-brown and was stirred at room temperature for 12 h. The reaction mixture was filtered through a Celite-padded coarse frit. The filtrate was collected, and the volatiles were removed under reduced pressure to give crude **12b** as a red-brown crystalline solid. Analytically pure samples of **12b** were obtained by recrystallization from a concentrated toluene solution at −30 °C (0.58 g, 0.64 mmol, 88%). ^{1}H NMR (toluene-d_8, 90 °C): δ 29.94 (br s, 4H, ortho H), 13.64 (t, J = 6.5 Hz, 2H, para H), 9.84 (br s, 4H, meta H), 8.46 (d, 4H, ortho H), 6.79 (t, J = 7.1 Hz, 2H, para H), 2.12 (br s, 4H, meta H), −1.54 (s, 30H, C_5(CH_3)$_5$), −2.94 (br s, 4H, CH_2Ph). UV−vis/NIR (ϵ, M^{-1} cm^{-1}, toluene): 312 (14 000), 380 (3700), 540 (600), 594 (480), 680 (240), 770 (160), 845 (35), 940 (35), 1022 (65), 1108 (25), 1178 (300), 1220 (390), 1369 (115). Mp = 204−205 °C. MS (EI, 70 eV): m/z 896 (M$^+$), 702 (M$^+$ − N=C(Ph)(Bz)). Anal. Calcd for $C_{48}H_{54}N_2$U (896.99 g/mol): C, 64.27; H, 6.07; N, 3.12. Found: C, 64.60; H, 6.19; N, 2.93.

Synthesis of (C₅Me₅)₂U[−N=C(Ph)(CH₃)]₂ (12c). A 125 mL Erlenmeyer flask equipped with a stir bar was charged with (C₅Me₅)₂U(CH₃)₂ (0.50 g, 0.93 mmol) and toluene (50 mL). To the resulting orange solution was added 0.245 mL of benzonitrile (0.247 g, 2.39 mmol) with stirring. The resultant reaction mixture changed color to a dark ruby red and was stirred at room temperature for 16 h. The volatiles were removed from the reaction mixture under reduced pressure to afford a foamy brown solid. This solid was taken up in hexanes (20 mL) and filtered through a Celite-padded coarse frit. The filtrate was collected, and the volatiles were removed under reduced pressure to give a red-brown solid. This solid was taken up in hexamethyldisiloxane (20 mL) and filtered through a Celite-padded coarse frit. Concentration of this hexamethyldisiloxane solution to ∼10 mL and storage at −30 °C affords analytically pure **12c** as a red-brown microcrystalline solid (0.495 g, 6.65 mmol, 71%). ^{1}H NMR (toluene-d_8, 91.7 °C): δ 17.15 (br s, 4H, ortho H), 12.44 (t, J = 7.1 Hz, 2H, para H), 6.40 (t, J = 7.1 Hz, 4H, meta H), −2.04 (s, 30H, C_5(CH_3)$_5$), −2.54 (br s, 6H, CH_3). UV−vis/NIR (ϵ, M^{-1} cm^{-1}, toluene): 306 (2200), 380 (1400), 540 (400), 640 (250), 840 (50), 934 (50), 982 (75), 1097 (220), 1175 (270), 1229 (335), 1350 (100). Mp = 116−117 °C. MS (EI, 70 eV): m/z 744 (M$^+$), 626 (M$^+$ − N=C(Ph)(Me)). Anal. Calcd for $C_{48}H_{54}N_2$Th·1/2NCC₆H₅

(796.36 g/mol): C, 59.58; H, 6.14; N, 4.49. Found: C, 59.51; H, 6.18; N, 4.16.

Crystallographic Details for (C₅Me₅)₂Th(CH₂Ph)₂ (9b). A pale yellow crystal (0.28 × 0.10 × 0.10 mm) grown from a concentrated hexanes solution of **9b** at −30 °C was mounted from Paratone N oil onto a glass fiber under argon gas flow and placed on a Bruker P4/CCD diffractometer, equipped with a Bruker LT-2 temperature device. A hemisphere of data was collected using φ scans, with 30 s frame exposures and 0.3° frame widths. A total of 18 073 reflections ($-11 \leq h \leq 11$, $-14 \leq k \leq 13$, $-28 \leq l \leq 29$) were collected at T = 203(2) K in the θ range 1.72−25.43° of which 5312 were unique (R_{int} = 0.0328); Mo Kα radiation (λ = 0.71073 Å). Data collection and initial indexing and cell refinement were handled using SMART^{36} software. Frame integration and final cell parameter calculations were carried out using SAINT^{37} software. The data were corrected for absorption using the SADABS program.^{38} Decay of reflection data was monitored by analysis of redundant frames. The structure was solved using direct methods, completed by subsequent difference Fourier techniques, and refined by full-matrix least-squares procedures. All non-hydrogen atoms were refined anisotropically, and hydrogen atoms were treated as idealized contributions. The absorption coefficient was 5.156 mm^{-1}. The least-squares refinement converged normally with residuals of R1 = 0.0404 ($I > 2\sigma(I)$), wR2 = 0.1286, and GOF = 1.058 (F^2); $C_{34}H_{44}$Th (684.73 g/mol), space group $P2_1/n$, monclinic a = 9.886(3) Å, b = 12.410(4) Å, c = 24.078(7) Å, α = 90°, β = 100.639(5)°, γ = 90°, V = 2903.1(14) Å^3, Z = 4, $F(000)$ = 1352, ρ_{calcd} = 1.567 g cm^{-3}. Structure solution, refinement, graphics, and creation of publication materials were performed using SHELXTL.^{39}

Crystallographic Details for (C₅Me₅)₂Th(CH₃)₂ (9c). A colorless crystal (0.24 × 0.10 × 0.08 mm) grown from a concentrated hexanes solution of **9c** at −30 °C was mounted from Paratone N oil onto a glass fiber under argon gas flow and placed on a Bruker P4/CCD diffractometer, equipped with a Bruker LT-2 temperature device. A hemisphere of data was collected using φ scans, with 30 s frame exposures and 0.3° frame widths. A total of 7884 reflections ($-9 \leq h \leq 10$, $-22 \leq k \leq 22$, $-11 \leq l \leq 11$) were collected at T = 203(2) K in the θ range 2.70−28.10° of which 2497 were unique (R_{int} = 0.0226); Mo Kα radiation (λ = 0.71073 Å). Data collection and initial indexing and cell refinement were handled using SMART^{36} software. Frame integration and final cell parameter calculations were carried out using SAINT^{37} software. The data were corrected for absorption using the SADABS program.^{38} Decay of reflection data was monitored by analysis of redundant frames. The structure was solved using direct methods, completed by subsequent difference Fourier techniques, and refined by full-matrix least-squares procedures. All non-hydrogen atoms were refined anisotropically, and hydrogen atoms were treated as idealized contributions. The disordered pentamethylcyclopentadienyl ligand was refined as two one-half occupancy positions (C3 through C12 and C3′ through C12′). The absorption coefficient was 6.852 mm^{-1}. The least-squares refinement converged normally with residuals of R1 = 0.0326 ($I > 2\sigma(I)$), wR2 = 0.0930, and GOF = 1.576 (F^2); $C_{22}H_{36}$Th (532.55 g/mol), space group $C2/c$, monclinic a = 8.3232(14) Å, b = 17.302(3) Å, c = 8.4939(15) Å, β = 117.185(3)°, V = 1088.1(3) Å^3, Z = 2, $F(000)$ = 516, ρ_{calcd} = 1.625 g cm^{-3}. Structure solution, refinement, graphics, and creation of publication materials were performed using SHELX-TL.^{39}

Crystallographic Details for (C₅Me₅)₂Th(−N=CPh₂)₂ (10a). An orange crystal (0.40 × 0.28 × 0.26 mm) grown from

(36) *SMART-NT 4*; Bruker AXS, Inc.: Madison, WI 53719, 1996.
(37) *SAINT-NT 5.050*; Bruker AXS, Inc.: Madison, WI 53719, 1998.
(38) Sheldrick, G. *SADABS*, first release; University of Göttingen: Germany.
(39) *SHELXTL* Version 5.10; Bruker AXS, Inc.: Madison, WI 53719, 1997.

a concentrated hexanes solution of **10a** was mounted from Paratone N oil onto a glass fiber under argon gas flow and placed on a Bruker P4/CCD diffractometer, equipped with a Bruker LT-2 temperature device. A hemisphere of data was collected using φ scans, with 30 s frame exposures and 0.3° frame widths. A total of 20 868 reflections ($-11 \leq h \leq 11$, $-22 \leq k \leq 22$, $-22 \leq l \leq 22$) were collected at $T = 203(2)$ K in the θ range 1.1−23.3° of which 10 444 were unique ($R_{int} = 0.0184$); Mo Kα radiation ($\lambda = 0.71073$ Å). Data collection and initial indexing and cell refinement were handled using SMART[36] software. Frame integration and final cell parameter calculations were carried out using SAINT[37] software. The data were corrected for absorption using the SADABS program.[38] Decay of reflection data was monitored by analysis of redundant frames. The structure was solved using direct methods, completed by subsequent difference Fourier techniques, and refined by full-matrix least-squares procedures. All non-hydrogen atoms were refined anisotropically, and hydrogen atoms were treated as idealized contributions. The absorption coefficient was 3.791 mm^{-1}. The least-squares refinement converged normally with residuals of R1 = 0.0337 ($I > 2\sigma(I)$), wR2 = 0.0601, and GOF = 2.092 (F^2); C$_{46}$H$_{50}$N$_2$Th (862.92 g/mol), space group $P\bar{1}$, triclinic $a = 10.640(4)$ Å, $b = 20.378(7)$ Å, $c = 20.555(7)$ Å, $\alpha = 64.241(5)°$, $\beta = 82.931(6)°$, $\gamma = 82.307(7)°$, $V = 3967(2)$ Å^3, $Z = 4$, $F(000) = 1720$, $\rho_{calcd} = 1.445$ g cm^{-3}. Structure solution, refinement, graphics, and creation of publication materials were performed using SHELXTL.[39]

Crystallographic Details for (C$_5$Me$_5$)$_2$Th[−N=C(Ph)-(Bz)]$_2$ (10b). A yellow-orange crystal ($0.10 \times 0.08 \times 0.08$ mm) grown from a concentrated hexanes solution of **10b** was mounted from Paratone N oil onto a glass fiber under argon gas flow and placed on a Bruker P4/CCD diffractometer, equipped with a Bruker LT-2 temperature device. A hemisphere of data was collected using φ scans, with 30 s frame exposures and 0.3° frame widths. A total of 9973 reflections ($-16 \leq h \leq 16$, $-14 \leq k \leq 14$, $-17 \leq l \leq 20$) were collected at $T = 203(2)$ K in the θ range 2.01−22.46° of which 2597 were unique ($R_{int} = 0.0948$); Mo Kα radiation ($\lambda = 0.71073$ Å). Data collection and initial indexing and cell refinement were handled using SMART[36] software. Frame integration and final cell parameter calculations were carried out using SAINT[37] software. The data were corrected for absorption using the SADABS program.[38] The structure was solved using direct methods, completed by subsequent difference Fourier techniques, and refined by full-matrix least-squares procedures. All non-hydrogen atoms were refined anisotropically, and hydrogen atoms were treated as idealized contributions. The absorption coefficient was 3.761 mm^{-1}. The least-squares refinement converged normally with residuals of R1 = 0.0615 ($I > 2\sigma(I)$), wR2 = 0.1135, and GOF = 1.273 (F^2); C$_{48}$H$_{54}$N$_2$Th (890.97 g/mol), space group $C2/c$, monoclinic $a = 15.416(5)$ Å, $b = 13.461(5)$ Å, $c = 19.347(6)$ Å, $\alpha = 90°$, $\beta = 94.673(6)°$, $\gamma = 90°$, $V = 4001(2)$ Å^3, $Z = 4$, $F(000) = 1784$, $\rho_{calcd} = 1.479$ g cm^{-3}. Structure solution, refinement, graphics, and creation of publication materials were performed using SHELXTL.[39]

Crystallographic Details for (C$_5$Me$_5$)$_2$U(CH$_2$Ph)$_2$ (11b). A green-black crystal ($0.14 \times 0.10 \times 0.06$ mm) grown from a concentrated hexanes solution of **11b** at −30 °C was mounted from Paratone N oil onto a glass fiber under argon gas flow and placed on a Bruker P4/CCD diffractometer, equipped with a Bruker LT-2 temperature device. A hemisphere of data was collected using φ scans, with 30 s frame exposures and 0.3° frame widths. A total of 14 577 reflections ($-11 \leq h \leq 11$, $-14 \leq k \leq 12$, $-28 \leq l \leq 28$) were collected at $T = 203(2)$ K in the θ range 1.72−25.45° of which 4871 were unique ($R_{int} = 0.0190$); Mo Kα radiation ($\lambda = 0.71073$ Å). Data collection and initial indexing and cell refinement were handled using SMART[36] software. Frame integration and final cell parameter calculations were carried out using SAINT[37] software. The data were corrected for absorption using the SADABS program.[38] Decay of reflection data was monitored by analysis of redundant

frames. The structure was solved using direct methods, completed by subsequent difference Fourier techniques, and refined by full-matrix least-squares procedures. All non-hydrogen atoms were refined anisotropically, and hydrogen atoms were treated as idealized contributions. The absorption coefficient was 5.720 mm^{-1}. The least-squares refinement converged normally with residuals of R1 = 0.0280 ($I > 2\sigma(I)$), wR2 = 0.0786, and GOF = 2.181 (F^2); C$_{34}$H$_{44}$U (690.72 g/mol), space group $P2_1/n$, monoclinic $a = 9.772(3)$ Å, $b = 12.328(4)$ Å, $c = 24.037(7)$ Å, $\alpha = 90°$, $\beta = 100.514(5)°$, $\gamma = 90°$, $V = 2847.2(15)$ Å^3, $Z = 4$, $F(000) = 1360$, $\rho_{calcd} = 1.611$ g cm^{-3}. Structure solution, refinement, graphics, and creation of publication materials were performed using SHELXTL.[39]

Crystallographic Details for (C$_5$Me$_5$)$_2$U(CH$_3$)$_2$ (11c). An orange crystal ($0.24 \times 0.16 \times 0.16$ mm) grown from a concentrated hexanes solution of **11c** at −30 °C was mounted from Paratone N oil onto a glass fiber under argon gas flow and placed on a Bruker P4/CCD diffractometer, equipped with a Bruker LT-2 temperature device. A hemisphere of data was collected using φ scans, with 30 s frame exposures and 0.3° frame widths. A total of 29 886 reflections ($-38 \leq h \leq 40$, $-31 \leq k \leq 41$, $-10 \leq l \leq 10$) were collected at $T = 203(2)$ K in the θ range 1.28−28.45° of which 5026 were unique ($R_{int} = 0.0320$); Mo Kα radiation ($\lambda = 0.71073$ Å). Data collection and initial indexing and cell refinement were handled using SMART[36] software. Frame integration and final cell parameter calculations were carried out using SAINT[37] software. The data were corrected for absorption using the SADABS program.[38] Decay of reflection data was monitored by analysis of redundant frames. The structure was solved using direct methods, completed by subsequent difference Fourier techniques, and refined by full-matrix least-squares procedures. All non-hydrogen atoms were refined anisotropically, and hydrogen atoms were treated as idealized contributions. The absorption coefficient was 7.609 mm^{-1}. The least-squares refinement converged normally with residuals of R1 = 0.0456 ($I > 2\sigma(I)$), wR2 = 0.0922, and GOF = 1.953 (F^2); C$_{22}$H$_{36}$U (538.54 g/mol), space group I_1/a, tetragonal, $a = 31.797(5)$ Å, $c = 8.438(3)$ Å, $V = 8532(3)$ Å^3, $Z = 16$, $F(000) = 4160$, $\rho_{calcd} = 1.677$ g cm^{-3}. Structure solution, refinement, graphics, and creation of publication materials were performed using SHELXTL.[39]

Crystallographic Details for (C$_5$Me$_5$)$_2$U[−N=C(Ph)-(Bz)]$_2$ (12b). A dark red crystal ($0.14 \times 0.10 \times 0.04$ mm) grown from evaporation of a concentrated toluene solution of **12b** was mounted from Paratone N oil onto a glass fiber under argon gas flow and placed on a Bruker P4/CCD diffractometer, equipped with a Bruker LT-2 temperature device. A hemisphere of data was collected using φ scans, with 30 s frame exposures and 0.3° frame widths. A total of 12 464 reflections ($-18 \leq h \leq 18$, $-16 \leq k \leq 16$, $-21 \leq l \leq 22$) were collected at $T = 203(2)$ K in the θ range 2.02−25.35° of which 3507 were unique ($R_{int} = 0.0256$); Mo Kα radiation ($\lambda = 0.71073$ Å). Data collection and initial indexing and cell refinement were handled using SMART[36] software. Frame integration and final cell parameter calculations were carried out using SAINT[37] software. The data were corrected for absorption using the SADABS program.[38] The structure was solved using direct methods, completed by subsequent difference Fourier techniques, and refined by full-matrix least-squares procedures. All non-hydrogen atoms were refined anisotropically, and hydrogen atoms were treated as idealized contributions. The absorption coefficient was 4.138 mm^{-1}. The least-squares refinement converged normally with residuals of R1 = 0.0236 ($I > 2\sigma(I)$), wR2 = 0.0550, and GOF = 1.208 (F^2); C$_{48}$H$_{54}$N$_2$U (896.96 g/mol), space group $C2/c$, monoclinic $a = 15.272(3)$ Å, $b = 13.469(3)$ Å, $c = 19.301(4)$ Å, $\alpha = 90°$, $\beta = 94.784(4)°$, $\gamma = 90°$, $V = 3956.3(14)$ Å^3, $Z = 4$, $F(000) = 1792$, $\rho_{calcd} = 1.506$ g cm^{-3}. Structure solution, refinement, graphics, and creation of publication materials were performed using SHELXTL.[39]

Supporting Information Available: Tables with bond lengths, bond angles, atomic coordinates, and anisotropic displacement parameters for the structures of **9b**, **9c**, **10a**, **10b**, **11b**, **11c**, and **12b**. This material is available free of charge via the Internet at http://pubs.acs.org.

OM0343824